IJME

Int. J. of Applied Mechanics and Engineering, 2024, vol.29, No.4, pp.61-77
DOI: 10.59441/ijame/192125

A PRACTICAL ALTERNATIVE MODEL TO APPROXIMATE A FULLY TWO DIMENSIONAL THERMALLY NON-SYMMETRIC ANNULAR FIN EFFICIENCY

Hadjira Benallel* and Mohamed Najib Bouaziz

Mechanical Engineering, Biomaterials and Transport Phenomena, ALGERIA
E-mail: benallel_h@yahoo.fr

A new practical and approximate two-dimensional is developed to take into account the thermally non-symmetric annular tick fin model and to avoid the laborious solution involving additional calculation of infinite eigenvalues. Using the perturbation method, a representative with satisfactory accuracy model is produced. For convenience, the developed analytical model is used here, in its numerical version, to show its validity and for an investigation of the effects of significant parameters on the efficiency of the annular fin. The same outcomes are obtained when the 1-D and present model are compared using the corresponding values. Then, different and easier calculations are carried out to illustrate the impact of the three primary parameters- the thickness, the asymmetry ratio, and the end Biot number- that define the annular fins. It is shown that, for thick or thin fins, the unequal convection heat coefficients of the two surfaces have a significant impact on the distribution temperature and fin efficiency. With high thermal conductivity thick fins can increase cooling efficiency. For thicker fins, a significant impact of the end Biot on fin efficiency is observed.

Key words: two-dimensional model, perturbation method, thickness annular fin, thermally non symmetric fin, fin efficiency.

1. Introduction

Intense heat transmission has been divided into active and passive techniques by Bergles [1]. Bergles and Manglik have also reported on the intensification of heat and mass transfer developments [2]. Applying them is helpful and required to obtain a high-performance apparatus. Passive methods are commonly utilized via fins and are less sophisticated than active systems, which require external power. The rate at which heat dissipates into the nearby cooling fluid is significantly increased by these increased surface areas. There is a vast range of uses. Fins are evidently used in heat exchangers, compressors, internal combustion engines, and biological wastewater treatment systems. Dissipating heat is essential for small systems, such integrated circuits, electronic components, and so on, in order to maintain the necessary reliability.

Because they are easy to make, the traditional varieties of these fins longitudinal, radial, annular, or spine configurations continue to be the focus of research in a large body of literature. These fins typically have a rectangular profile. The previous thirty years have seen a number of advancements and changes brought about by growing demand from a variety of applications, space limitations, and new operating conditions. Maji and Choubey [3] reported some advancements in plate fins, pin fins, perforated fins, and porous fins in addition to fins having profiles other than rectangular or classical fins. Elliptical annular fins were reviewed by Nagarani *et al.* [4]. Utilizing more annular fins in a thermal storage that stores latent heat, adding fins significantly enhances the system's performance, Tiari *et al.* [5]. In a more recent paper, Zhang *et al.* [6] provide a thorough prospective analysis of phase change materials utilized. They point out that other enhancement techniques including nanofluids, metal foam, and ultrasonic vibrations can be used to improve the heat transfer of the latent thermal energy storage system using an extended surface area, such as the annular fins.

* To whom correspondence should be addressed

Optimizing the weights and prices of the finned system is crucial since the type, number, and configuration of the concrete project lead to a large amount of material with high thermal conductivity. A high technical parameters are decide for the design of a fundamental fin. The fin efficiency which is determined by the temperature distributions at every location along the device often makes a difference.

Around the axis, the annular fins are organized into concentric rings. They encircle the fluid flow in concentric circles. Applications needing intense cooling, such high-power electronic systems and semiconductor devices, can employ these kinds of fins. Additionally, they can provide a useful solution in cases where a significant heat exchange surface area is needed when space is at a premium. An annular fin is more efficient than a radial fin when heat movement is predominantly axial, as in centrifugal compressors. It can be very useful in capturing and dissipating heat in these kinds of applications. A more or less complex modeling of the annular fin's heat transfer process with its surrounding environment needs to be created in order to lower the cost of experiments. Therefore, the governing differential equation related to boundary conditions is solved mathematically. Nonetheless, the model's nature determines which approach – analytical, numerical, or semi-analytical – to use and may differ from models based on one or more unrealistic assumptions.

Numerous books and articles, both recent and old, have examined the application of classical fins. Closed-form solutions exist [7] and with analysis [8-11] where conduction is according to one direction in an annular fin constant thickness and the boundary conditions describing the heat transfer process are linear. An approximate analytical approach has been proposed by Campo *et al.* [12] to make the solution resemble a longitudinal fin. Fins that are thicker have a higher thickness relative to height. They provide higher heat dissipation from forced convection, superior thermal conduction, and mechanical resistance against stress and vibration, making them somewhat favored over thin fins in some situations. Derivation of accurate formulas for the two-dimensional temperature distribution in the annular fin has received attention over the years. According to Kraus *et al.* [10], the majority of heat transfer literature give the precise solution involving modified first and second-kind Bessel functions and infinite eigenvalues. Depending on the required number of terms, the calculation of the solution is laborious in order to acquire an accurate numerical solution. Examining the calculation's sensitivity and ensuring grid convergence in the model are two ways to assess accuracy. Nellis and Klein [13] provide a clear example illustration of the 2-D temperature distribution inside the straight fin. You'll see that the eigenvalues are rarely obtained analytically. A small number of eigenvalues can be used to simplify the analytical solution under certain conditions, allowing for simpler numerical computations [7].

In order to circumvent this, considerable investigation was done to identify a qualitative standard that allows the 1-D expressions to remain valid while taking the 2-D annular fins into account. The relative errors between using 1-D and 2-D solutions have been graphically depicted by Lau and Tan [14], Heggs and Stone [15]. The inaccuracy for the first authors increases to *50%* for aspect ratios larger than unity and for $Bi = 10$. Further limitations on the Biot number have been discovered by Snider and Kraus [16]. Limitations on the aspect ratio and transverse Biot number order were acknowledged by Razelos and Georgiou [17]. Other approaches, such as a new technique or a technical transform methods to provide alternative formulations [18-21] for longitudinal fins and limited computations for circular annular fins [7], have been used to modify the 2-D formulation.

When modeling a fin, under some assumptions, this real distinction between one and two dimensions, is not the only problem, and in general, the quantities of interest are derived and calculated using analytical, semi-analytical, and numerical solutions. To date, experimental results are becoming increasingly rare when compared to numerical results as in [22]. The complete employment of digital tools is most common when fin geometries are complicated and fit into sets of systems. For example, [23] simulated the solidification process of PCMs in a heat exchanger with circular cross-section using branched-shaped fins. Using CFD, a fin assembly can be modeled as a porous medium [24]. In some cases, the fin is only treated as a boundary condition for fluid flow [25]. When high precision is required, entire discretization is implemented, as showed in [26-29] for high coupled and conjugate problems. Durgam *et al.* [30] examined the heat transfer rate, focused on the fins with different materials, whereas Sobamowo [31] employed FEM (finite elements method) for moving porous fins. The heat transfer coefficient can also be estimated using advanced FEA (finite elements analysis) [32].

Newer research methods, including the heat transfer, are widely used on the fins areas. The approximate analytical methods such as HPM (homotopy perturbation method), HAM (homotopy analysis

method), LSM (least square method), DTM (differentiel transform method), DIM (Daftardar-Gejiji and Jarari method), Haar wavelet collocation technique, Chebyshev collocation spectral approaches, ASM (Ananthaswamy-Sivasankari method), and others are used to solve complex problems with high nonlinearities, coupled phenomena in fins, and with more variety of configurations as in [33-37].

The phenomenological convective heat transfer coefficient is frequently taken to have a constant value in fin literature. Because of the intricate relationship that exists between the surrounding fluid and the device, this simplification is not always accurate. In actuality, if the fluid's characteristics fluctuate significantly, it is not only space-dependent but also temperature-dependent. Due to the important roles played by the leading edge, boundary layer, and turbulence, the heat transfer rate varies along the whole length. Additionally, standard analysis or empirical correlations must be used to estimate the convective transfer coefficient beforehand. Because the height fin is not particularly very large, an overall coefficient can be applied for each face. However, values can differ significantly from one side to the other. Look [38] pointed out that when asymmetrical convective transfer coefficients are present, the standard one-dimensional assumption is especially incorrect. There could be a discrepancy bigger than a factor of two. In their articles, Look [38-39] and Look and Kang [40-41] discussed the impact of uneven coefficients in 2-D longitudinal fin formulations. Kang and Look [42] looked at a thermally asymmetric triangular fin for the same analysis. Based on a 2-D mathematical formulation, these researches were extended for a rectangular fin by Kang and Look [43] in the case of convective annular fins, and by Kang and Look [44] for optimization of convective-radiating annular fins. It is significant to note that temperature distributions and heat loss were calculated using two hundred terms and five eigenvalues for each change of the parameters. Chang and Chen [45] examine the 2-D annular fin's transient response using the Laplace transform. Analytical solutions for orthotropic annular fins are given by Mustapha *et al.* [46].

This work aims to provide a realistic and approximate solution for a two-dimensional annular fin that is not exposed to the same convective heat transfer coefficients at its faces and tip-fin. Il should be noted that in the classical models 1-D or 2-D, the fin is under a thermally symmetric assumption. Initially, the perturbation method reduces the 2-D mathematical representation of the thin or thick fin that will be easy to solve. As a result, the present solution of the annular fin is expected more practical and consistent with physical reality. The tip-fin heat transfer coefficient is not regarded as negligible as in thick fin, is taken into consideration. In addition, this alternate approach have the advantage of accurately solving the temperature distribution and efficiency for thermally non-symmetric annular fin, both for thin and thick fins.

2. Statement and formulation of the problem

Examine the physical scenario of interest, which is represented by the two-dimensional rectangular annular and fixed fin (this device do not turn around the *z*-axis), in Fig.1, that dissipates heat to a surrounding fluid by convection and has a constant thermal conductivity λ of isotropic and homogenous material. The constant thickness *w*, the outer radius r_b, and the inner radius r_a are the geometrical dimensions. While portion of the heat from the inner heat fluid naturally flows in the *z*-axis and *r*-axis perpendicularly to the annular fin base and tube wall, the rest of the heat moves with fluid flows in the *z*-axis vertically in the pipe. The circumferential surface convection heat transfer coefficient are h_1 for the annular fin's bottom surface, h_2 for the top surface, and a non-negligible h_3 for the fin tip that is not always insulated. Considering that the convection heat transfer coefficients are all constant but noticeably different on opposite sides. When compared to the corresponding Murray-Gardner assumption, this scenario with thermally non-symmetric (or asymmetrical values of h_1 and h_2 relative to the plane $z = 0$) fin is more plausible [8]. Furthermore, there is no internal radiation mode or heat generation. The ambient temperature is T_∞, and the temperature at the fin base is T_a.

The governing equation for the temperature distribution along the described annular fin, is

$$\frac{\partial}{\partial r}\left(-\lambda\frac{\partial T}{\partial r}\right)+\frac{1}{r}\left(-\lambda\frac{\partial T}{\partial r}\right)+\frac{\partial}{\partial z}\left(-\lambda\frac{\partial T}{\partial z}\right)=0\,. \tag{2.1}$$

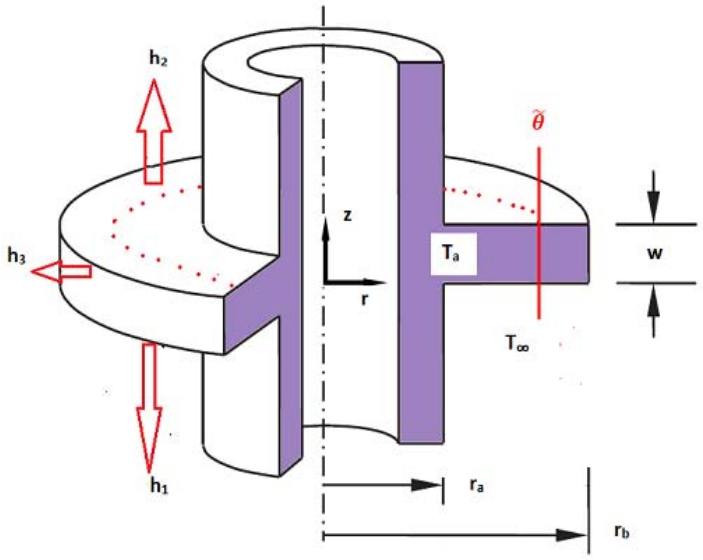

Fig.1. Schematic of a rectangular profile 2-D thermally non-symmetric annular fin.

The heat flows in both directions are written as follows:

$$q_r = -\lambda \frac{\partial T}{\partial r}, \qquad q_Z = -\lambda \frac{\partial T}{\partial z}. \tag{2.2}$$

In accordance with the non-symmetric nature of the heat exchanges, the thermal boundary conditions at the fluid-annular fin interfaces are:

$$r = r_a, \quad T = T_a, \tag{2.3}$$

$$r = r_b, \quad -\lambda \frac{\partial T}{\partial r} = h_3 \left(T - T_\infty\right), \tag{2.4}$$

$$z = 0, \quad -\lambda \frac{\partial T}{\partial z} = -h_1 \left(T - T_\infty\right), \tag{2.5}$$

$$z = w, \quad -\lambda \frac{\partial T}{\partial z} = h_2 \left(T - T_\infty\right) \tag{2.6}$$

where, T is the fin-temperature.
In order to make the above equations dimensionless, the following non-dimensional parameters are introduced

$$\theta = \frac{T - T_\infty}{T_a - T_\infty}, \quad R = \frac{r}{r_b}, \quad Z = \frac{z}{w}, \quad \delta = \frac{w}{r_b}, \quad c = \frac{r_a}{r_b}. \tag{2.7}$$

Then, Eqs (2.1)-(2.6) are written as:

$$\frac{\partial^2 \theta}{\partial R^2} + \frac{1}{R}\frac{\partial \theta}{\partial R} + \frac{\partial}{\partial Z}\left(\frac{1}{\delta^2}\frac{\partial \theta}{\partial Z}\right) = 0, \tag{2.8}$$

or, in terms of dimensionless heat flows

$$\frac{\partial}{\partial R}(q_R)+\frac{1}{R}(q_R)+\frac{\partial}{\partial Z}(q_Z)=0 \tag{2.8a}$$

where

$$q_R=-\frac{\partial\theta}{\partial R} \quad \text{et} \quad q_Z=-\frac{1}{\delta^2}\frac{\partial\theta}{\partial Z}. \tag{2.9a-2.9b}$$

And the boundary conditions become

$$R=c, \quad \theta=1, \tag{2.10}$$

$$R=1, \quad -\frac{\partial\theta}{\partial R}=\frac{Bi_3}{\delta}\,\theta, \tag{2.11}$$

$$Z=0, \quad -\frac{\partial\theta}{\partial Z}=-Bi_1\theta, \tag{2.12}$$

$$Z=1, \quad -\frac{\partial\theta}{\partial Z}=Bi_2\theta. \tag{2.13}$$

The dimensionless Biot numbers are defined as:

$$Bi_1=\frac{h_1 w}{\lambda}, \quad Bi_2=\frac{h_2 w}{\lambda}, \quad Bi_3=\frac{h_3 w}{\lambda}. \tag{2.14}$$

3. Reduction of the system by perturbation method

Physical dimensionless temperature and heat flow are expressed a priori in zero and first orders terms:

$$\theta=\theta_0+\delta^2\theta_1, \tag{3.1}$$

$$q_R=q_{R0}+\delta^2 q_{R1}, \tag{3.2}$$

$$q_Z=q_{Z0}+\delta^2 q_{Z1} \tag{3.3}$$

here δ is the dimensionless fin thickness that is adopted as the parameter of perturbation.
Substituting Eqs (3.1), (3.3) and (2.9b) in one part, and Eqs (3.1), (3.2) and (2.9a) in other part; by identification gives

$$\frac{\partial\theta_0}{\partial Z}=0 \quad \text{and} \quad q_{Z0}=-\frac{\partial\theta_1}{\partial Z}, \tag{3.4}$$

$$q_{R0}=-\frac{\partial\theta_0}{\partial R}. \tag{3.5}$$

Substituting again Eqs (3.1), (3.3) and (2.8a) shows that $\frac{\partial q_{Z0}}{\partial Z}$ is in dependence only with *R*, so

$$\frac{\partial q_{Z0}}{\partial Z} = f(R) \text{ or by integrating } q_{Z0} = f(R).Z + g(R). \tag{3.6}$$

From Eqs (3.4) and (3.6) $-\theta_1 = f(R)\frac{Z^2}{2} + g(R)Z + h(R)$. (3.7)

This last equation (3.7) is replaced into Eq.(3.1), while Eq.3.6) is replaced into Eq.(3.3)

$$\theta = \theta_0 - \delta^2\left[f(R)\frac{Z^2}{2} + g(R)Z + h(R) \right] \tag{3.8}$$

$$q_Z = q_{Z0} + \delta^2 q_{Z1} = f(R)Z + g(R) + O\left(\delta^2\right). \tag{3.9}$$

The functions f, g and h are still unknown.

Now, an average temperature $\left(\tilde{\theta}\right.$ in figure $\left.1\right)$ along the *Z*-axis is sought, and by integration of Eq.(3.8)

$$\tilde{\theta} = \int_0^1 \theta(R,Z)\,dZ = \theta_0 - \delta^2\left[f(R)\frac{1}{6} + g(R)\frac{1}{2} + h(R) \right], \tag{3.10}$$

or $$\theta_0 = \tilde{\theta} + \delta^2\left[f(R)\frac{1}{6} + g(R)\frac{1}{2} + h(R) \right]. \tag{3.10a}$$

Finally, the Eq.(2.8) is reduced to 1-D differential equation:

$$\frac{\partial^2\tilde{\theta}}{\partial R^2} + \frac{1}{R}\frac{\partial\tilde{\theta}}{\partial R} - f(R) = 0. \tag{3.11}$$

The boundary conditions applied to Eqs (2.12) and (2.13) with the help of Eq.(3.10a), form a system:

$$\frac{Bi_1}{6}f + \left(1 + \frac{Bi_1}{2}\right)g = -\frac{Bi_1}{\delta^2}\tilde{\theta} \quad \text{and} \quad \left(1 + \frac{Bi_2}{3}\right)f + \left(1 + \frac{Bi_2}{2}\right)g = \frac{Bi_2}{\delta^2}\tilde{\theta}.$$

Which is resolved for the unknown *f* and *g*

$$f = \frac{12\left(Bi_1 + Bi_2 + Bi_1Bi_2\right)}{\left(12 + 4Bi_1 + 4Bi_2 + Bi_1Bi_2\right)}\frac{\tilde{\theta}}{\delta^2} \quad \text{and} \quad g = \frac{-6Bi_1\left(2 + Bi_2\right)}{\left(12 + 4Bi_1 + 4Bi_2 + Bi_1Bi_2\right)}\frac{\tilde{\theta}}{\delta^2}. \tag{3.12}$$

Then, the reduced 2-D differential equations will be:

$$\frac{\partial^2\tilde{\theta}}{\partial R^2} + \frac{1}{R}\frac{\partial\tilde{\theta}}{\partial R} - \frac{\beta}{\delta^2}\tilde{\theta} = 0 \tag{3.13}$$

where

$$\beta = \frac{12\left(Bi_1 + Bi_2 + Bi_1 Bi_2\right)}{12 + 4Bi_1 + 4Bi_2 + Bi_1 Bi_2}.$$

Equation (3.13) is completed by the boundary conditions, Eqs (2.10) and (2.11), which together form a differential system that approximate the 2-D thermally non-symmetric annular fin with fin tip that experiences no negligible heat loss, under a complex convective heat transfer coefficient β. In this presentation, β appearing denotes as a complex Biot number by the combination of Bi_1 and Bi_2, and highlighted δ the dimensionless thickness of the annular fin.

The annular fin efficiency can be determined by differenciation of $\tilde{\theta}(R)$ at the fin base

$$\eta = -\frac{2c}{1-c^2}\frac{\delta^2}{\beta}\frac{d\tilde{\theta}}{dR}. \tag{3.14}$$

4. Variations of the complex coefficient β

Let's introduce the parameter $\gamma = \frac{Bi_2}{Bi_1}$, that shows the effects of equality/unequality of the top to the bottom Biot numbers, β can be rewritten more suitably and expressively as

$$\beta = \frac{12\,Bi_1\left(1 + \gamma + Bi_1\gamma\right)}{12 + Bi_1\left(4 + 4\gamma + Bi_1\gamma\right)}. \tag{3.15}$$

Figures 2a, 2b, and 2c show the variations of the complex coefficient β with Bi_1 for particular values of the parameter $\gamma = [0, 0.5, 1, 5]$. When the complex coefficients in the models labelled present 2-D and classical 1-D formulations are plotted with Bi_1 in the practical range of $[0-0.1]$, as shown in Fig.2a, and for $\gamma = 1$, they are identical. Naturally, it should be mentioned that here, $\beta = 2Bi_1 = 2Bi_2$. Because the two models prescribe the identical physical description for the convection heat transfer coefficients in this basic situation. In this case, conductive heat transfers within the annular fin predominate over convective heat transfers to the surrounding environment, then, the current modeling appears to be valid for this range of low Biot values.

It is observed that when β is smaller than $2Bi_1$ in the scenario when γ is less than unity, illustrates the fin's two faces' thermal disparity, which is technically compatible with different heat exchange. Also take note of the fact that a reduction in β is theoretically possible in the extreme situation, denoted by $\gamma = 0$, which indicates that there is no heat exchange from the fin's upper face.

Conversely, in more real-world scenarios, $\gamma > 1$, and for example $\gamma = 5$, Fig.2a employs and displays a significant growth of β to indicate unfavorable cases relative to previous case.

The similar patterns are seen in Fig.2b for the Bi_1 range of $[0-0.1]$. As a limit criterion for the employment of the classical 1-D model, a difference between the two models for the classic case can be kept, beginning at $Bi_1 = 0.1$. This result, with the Biot number equal to *0.2* based on half the thickness, strictly satisfies the 1-D model's validity limit [7]. It should be emphasized that beyond this limit value, the 1-D model, which is always based on $2Bi_1$, becomes unrepresentative of the annular fin's thermal exchanges. For equal or unequal Bi_1 and Bi_2, this can be explained by ignoring the axial heat fluxes along the *z*-axis.

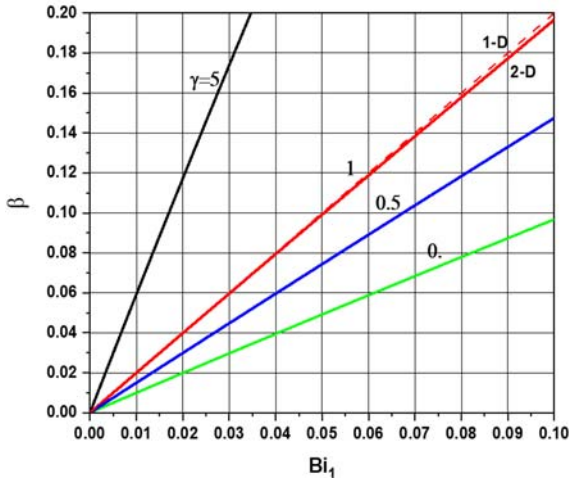

Fig.2a. Variations of β with $Bi_1\ [0-0.1]$ for different γ.

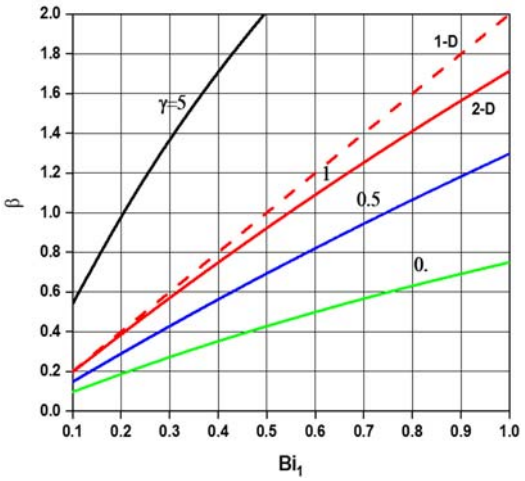

Fig.2b. Variations of β with $Bi_1\ [0.1-1.]$ for different γ.

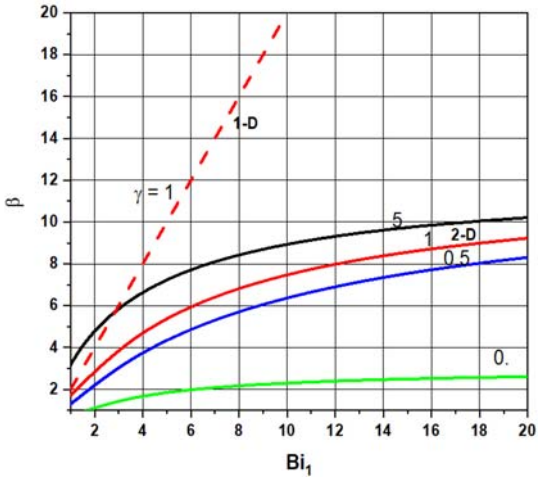

Fig 2c. Variations of β with $Bi_1\ [1.-20.]$ for different γ.

Conversely, in more real-world scenarios, $\gamma > 1$, and for example $\gamma = 5$, Fig.2a employs and displays a significant growth of β to indicate unfavorable cases relative to previous case.

The similar patterns are seen in Fig.2b for the Bi_1 range of $[0-0.1]$. As a limit criterion for the employment of the classical 1-D model, a difference between the two models for the classic case can be kept, beginning at $Bi_1 = 0.1$. This result, with the Biot number equal to *0.2* based on half the thickness, strictly satisfies the 1-D model's validity limit [7]. It should be emphasized that beyond this limit value, the 1-D model, which is always based on $2Bi_1$, becomes unrepresentative of the annular fin's thermal exchanges. For equal or unequal Bi_1 and Bi_2, this can be explained by ignoring the axial heat fluxes along the *z*-axis.

Therefore, it seems that as Bi_1 increases, β is comparatively smaller for all values of γ that describe the current 2-D model, and they no longer have a straight course. However, in accordance with the realistic thermal phenomenon, there is less error when heat flows are included along the vertical axis. Figure 2c illustrates the continuation of this pattern from $Bi_1 = 2$ until the asymptotic limits of β are reached. For example, for

$Bi_1 = 20$, the recorded couples (β, γ) of values are $\left[(10, 5); (9, 1); (8, 0.5) \text{ and } (2.7, 0)\right]$. When $Bi_1 \to \infty$, the absolute limits are $\beta = 12$ for all values of $\gamma \neq 0$ and $\beta = 12$ if $\gamma = 0$.

5. Validation of the model

For classical 2-D model annular fin formulation, as previously mentioned, closed-form solutions are available; nevertheless, the computations are laborious and impractical. The present analytical model can be used more simply despite more general physical considerations. To facilitate investigations, the numerical implementation of this model is chosen here. Numerical findings covering the fin temperature distribution scale are displayed in Fig.3 using the already created realistic present model that accounts for both the non-symmetric thermally annular fin problem and the heat transfer fluxes down the *z*-axis. The @Matlab code bvp4c makes it easier to solve system Eqs (3.13), (2.10), and (2.11). The code utilizes an implicit class of the Lobatto method and is based on the finite difference methodology.

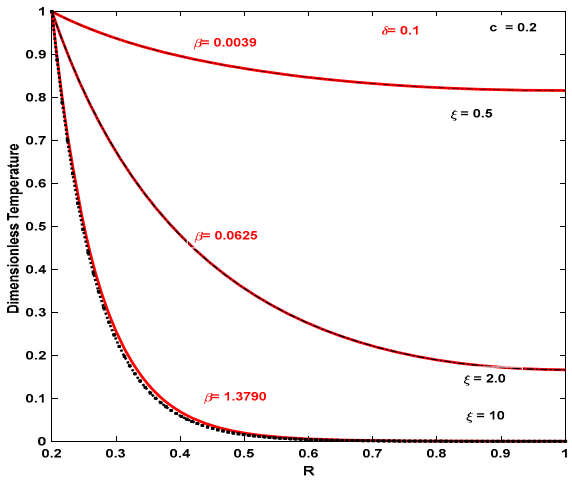

Fig.3 Comparisons with dimensionless temperature.
(in red: present model) and (in black: 1-D model, Campo *et al.*[12])

In order to guarantee that the results fully satisfy the boundary conditions, a convergence threshold of 10^{-4} was chosen for the mesh, and the calculations were carried out starting with an initial solution vector. The numerical results are compared with the exact temperature distributions, for small radius $(c = 0.2)$, $(Bi_3 = 0)$, $\gamma = 1$, and relatively thin fin $(\delta = 0.1)$, for differents dimensionless- geometrical fin parameters, as in [12]. It should be noted that here, the term $\dfrac{\xi^2}{\left(1-c^2\right)}$ is equivalent to $\dfrac{\beta}{\delta^2}$ for the two different formulations. It is important, of course, to note that ζ is calculated by a Biot number based on half of the thickness of the fin. Consequently, the Biot number Bi_1 considered in the present 2-D model must be twice than in the 1-D model, as reported in the Figs 2a-2c, to access β.

As can be seen in Fig.3, the two sets of data agree fairly well, except for the larges values of β and its equivalent the enlarged Biot number ζ. This can be attributed to the difference observed between the two models, as explained in Figs 2a, 2b, showing the variations of $2Bi_1$ (1-D model) and the corresponding ones of β. Beyond a certain value of β, the two models begin to diverge, limiting the accuracy of using the classic 1-D model.

6. Results and discussion

The current model was used to do several calculations for a few typical values of the parameters affecting the temperature distribution and, in turn, the annular fin's efficiency.

6.1. Effect of the thickness δ

In comparison to Fig.3, Fig.4 is set up to track the temperature distributions with thicker annular fins $(\delta = 0.3$ and $0.6)$. The evolution of the curves is displayed below for $\gamma = 1$ and three distinct and arbitrary values of β. The thicker annular fins have more favorable temperature distributions than the narrower ones for every value of β. The graph corresponding to $\delta = 1$ is reported for $\beta = 0.4$.

Therefore, thick fins with high thermal conductivity can improve cooling efficiency by providing a larger surface area for heat exchange from the inner fluid to the fin when high heat dissipation is needed. In fact, in the case of intense applications or low natural convection, this is the only option to get greater heat dissipation. Furthermore, thick fins can offer greater mechanical strength, which is beneficial in situations when there is mechanical stress, vibration, or shock.

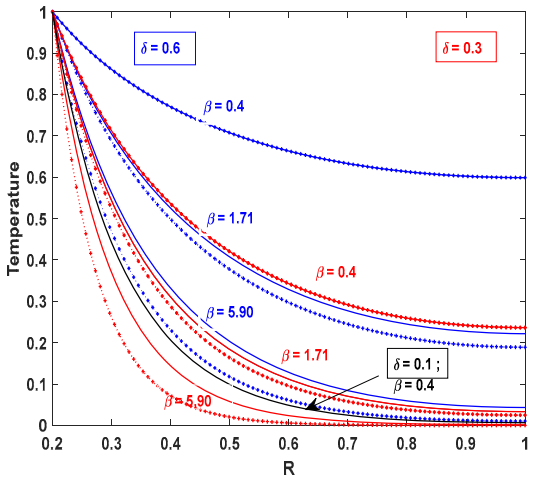

Fig.4 Effect of relative thickness δ on dimensionless temperature; $\gamma = 1$.
(by present model): blue $\delta = 0.6$; red $\delta = 0.3$; black $\delta = 0.1$,
(by 1-D model): red..... $\delta = 0.3$; blue..... $\delta = 0.6$.

Interestingly, as this Fig.4 illustrates, for large values of β, there is a significant increase in the difference between the 1-D model and the current model. Figure 3 previously reported this difference, which was not significant for $\delta = 1$. This discrepancy demonstrates how the current model, with its progressively thick and primarily convective fins, differs from the traditional 1-D model. These outcomes support the conclusions in [7, 14].

6.2. Effect of γ

For $\delta = 0.1$ in Fig.5 and 0.3 in Fig.6, the effects of the annular fin's primary surfaces that do not convect with the same Biot numbers are displayed. In Fig.2a, the values selected for the number of Bi_1 (*0.05*, *0.5*, and *0.005*) are quite low, which aligns with the low values of β. To keep things simple, the end Biot Bi_3 is set to *0*. In practical terms, this encompasses the area of fins utilized in numerous applications. However, the computations are done for four retained γ values, *0*; *0.5*; *1* and *5*, in order to emphasize the inequality of transfers from the upper and lower faces of the fins.

These figures demonstrate how important the non-symmetric thermal fin is. Because of the weight of heat exchanges towards the upper face, one may see an improvement in the temperature distributions for values less than unity on both sides of the classic curves $(\gamma = 1)$. The heat dissipation, which is more advantageous in the positive vertical *Z*-direction, can explain this. If $\gamma > 1$, not beneficial dimensionless temperature is observed. This outcome is consistent with the experimenters' findings [10, 38], which shows that when the fin exchanges regime is by natural convection, the average transfer coefficient of the upper face is twice that of the lower face.

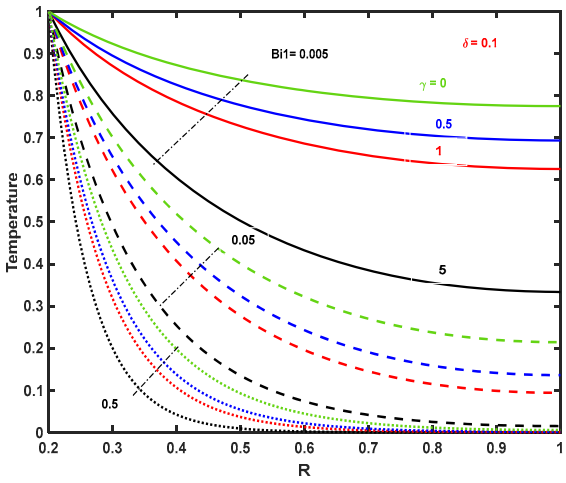

Fig.5. Effect of γ on dimensionless temperature for different Bi_1; $\delta = 0.1$.

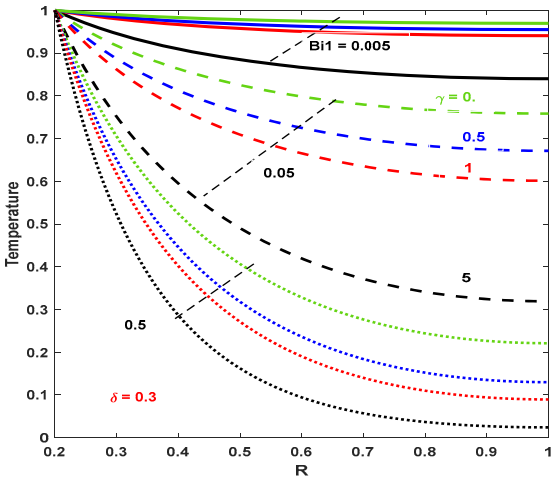

Fig.6. Effect of γ on dimensionless temperature for different Bi_1; $\delta = 0.3$.

6.3 Effect of Bi_3

No change happens when the fin is insulated $(Bi_3 = 0)$ or under a larger tip condition for $Bi_1 = 0.5$ and $\delta = 0.1$. Physically speaking, this is explained by the small surface area available for convection.

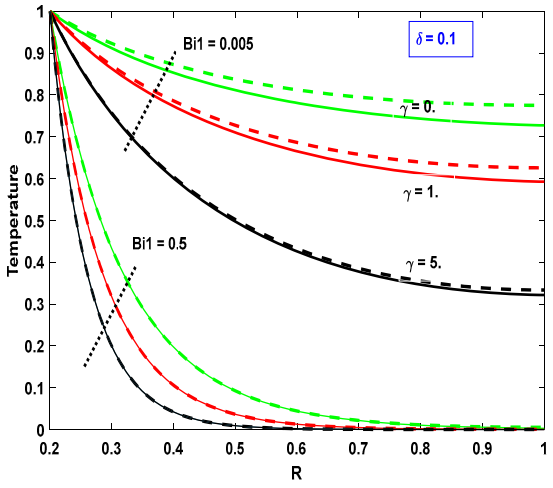

Fig.7. Effect of Bi_3 on dimensionless temperature for different Bi_1 and γ; $\delta = 0.1$; —— $Bi_3 = Bi_1$; ------ $Bi_3 = 0$.

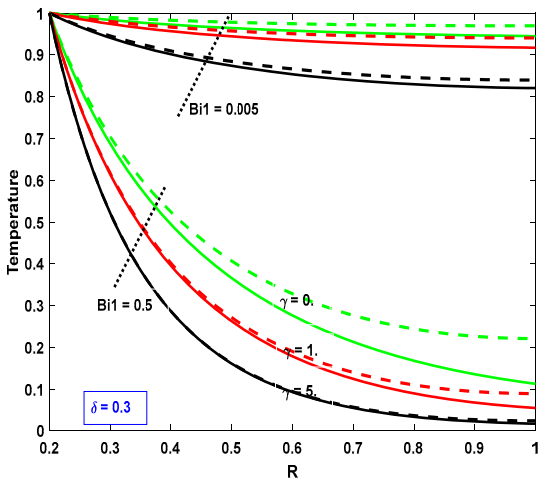

Fig.8. Effect of Bi_3 on dimensionless temperature for different Bi_1 and γ; $\delta = 0.3$; —— $Bi_3 = Bi_1$; ------ $Bi_3 = 0$.

Significant variations are observed at the opposite $(Bi_1 = 0.005)$, and for $\gamma < 1$, where the convection coefficient is lower, as inferred from fin efficiency [7]. It is obvious that altering the uneven Biot numbers can be a useful tool for managing and enhancing the annular fin's performance in situ. For large uneven surfaces with high Biot values, these impacts are particularly pronounced (Fig.7). Figure 8, fitted for a fin with $\delta = 0.3$, shows that even for larger convection coefficients, the fin tip state has a greater influence on the thermal characteristics of a fin. It is evident that an annular fin interacts with its environment more than a narrow fin does through a thick surface.

6.4. Efficiency

The annular fin efficiency versus Bi_1 are shown using Eq.(3.14). With $c = 0.2$ and $\delta = 0.1$ and 0.3 fixed, Fig.9 is only based on an insulated fin, whereas Fig.10 takes into account varying Bi_3. It is evident that thicker fins yield higher efficiency than thin fins.

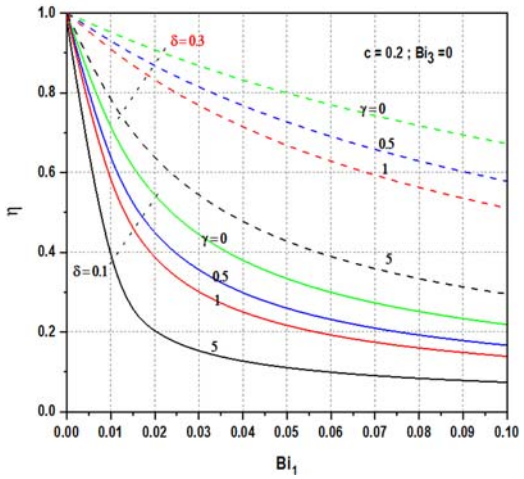

Fig.9. Fin efficiency versus radial Bi_1 and γ $(\delta = 0.1$ and $\delta = 0.3)$; $Bi_3 = 0$.

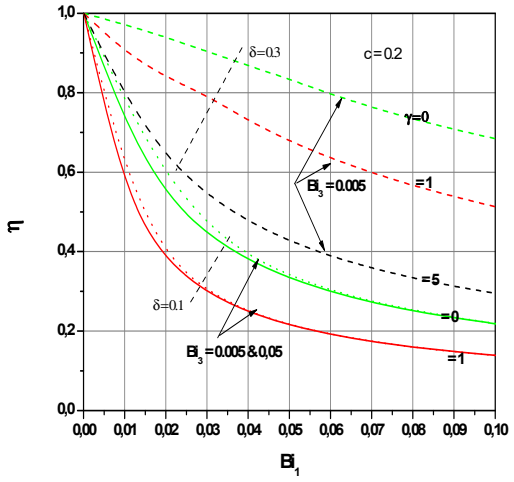

Fig.10. Fin efficiency versus radial Bi_1 and γ for different Bi_3 $(\delta = 0.1$ and $\delta = 0.3)$.

It is clear that, across all curves, a rise in Bi_1 is correlated with a fall in fin efficiency. Different in Bi_3 for constant γ have no discernible impact on fin efficiency for all thin fins, but for thicker fins, great difference occurs when γ varies significantly (Fig.10). This highlights the significance of the thermal inequality of the Biot number combined with the thick or thin annular fin, with or without convection at the end. It is necessary to keep these findings in mind when building such devices and/or enhancing their functionality.

7. Conclusion

The thick fins should be of interest to a wide range of applications where either a substantial amount of heat dissipation over a relatively big surface is required, or where intensive cooling is advised. The closed form analytical solution for these fins does not permit asymmetry of heat exchanges on the two faces and is characterized by tedious calculation. Here, a useful two-dimensional model that considers the thermally non-symmetric annular fin is constructed and reduced to a 1-D equivalent model using the perturbation approach. The model solution, which was swiftly computed using a @Matlab' bvp4c solver, can be used to emphasize the following results of this study:

1. The current practical model is verified for thin fins, yielding different dimensionless temperature when taking greater Biot numbers into consideration, and giving the same findings estimated by the classic 1-D model.
2. The results obtained by this model take into account transverse heat transfers within the fin, particularly for thick ones.
3. A thick annular fin outperforms a thin fin in efficiency, as predicted.
4. The dimensionless temperature and annular fin efficiency are significantly impacted by the non-symmetric Biot numbers ratio. Consequently, it is possible to view the unequal Biot numbers as a useful tool for managing and enhancing the extended surfaces' performance in their current location.
5. Even for low or higher non-symmetric convection coefficients, the fin tip condition has a greater impact on the thermal characteristics of the fin.
6. The current approximation model is anticipated to be helpful without laborious computations for the thermal design of thick annular fins and their efficiency, primarily for special applications that necessitate strong heat extraction via annular fins.
7. This practical model can be substituted for the classic 2-D model, not only for thick or thin annular fins. In addition, due to its simple calculation, it supports a thermally non-symmetric convection coefficients of the faces.

In practice of designing systems equipped with fins, the wide use today of simulation software, most of the time considers the fin as a boundary condition. Due to the fluid-fin interaction, the conjugate problem is necessary to obtain reliable results. To this end, future works must be carried out for other fin geometries and propose them as modules of choice to integrate them into CFDs.

Acknowledgements

This work was supported by the Biomaterials and transport phenomena laboratory, agreement N° 303 03-12-2003, at University Yahia Fares of Medea. The authors acknowledge and gratefully thank the financial support provided by the DG-RSDT of Algeria and appreciate the constructive comments of the reviewers which led to definite great improvement in the paper.

Nomenclature

Bi_1 – Biot number of down surface

Bi_2 – Biot number of upper surface

Bi_3 – end fin Biot number

c – dimensionless radius ratio

f, g, h – auxiliary functions

h_1 – convective heat transfer coefficient down surface

h_2 – convective heat transfer coefficient upper surface

h_3 – convective heat transfer coefficient at end fin

q_r – heat flux in *r*-direction

q_R – dimensionless heat flux in *r*-direction

q_{R0} – dimensionless heat flux in *r*-direction, zero-order

q_{R1} – dimensionless heat flux in *r*-direction, first-order

q_z – heat flux in *z*-direction

q_Z – dimensionless heat flux in *Z*-direction

q_{Z0} – dimensionless heat flux in *Z*-direction, zero-order

q_{Z1} – dimensionless heat flux in *Z*-direction, first-order

r – cylindrical coordinate

r_a – inner radius

r_b – outer radius

R – dimensionless cylindrical coordinate

T – fin temperature

T_a – fin base temperature

T_∞ – ambient temperature

w – fin thickness

z – vertical coordinate

Z – dimensionless vertical coordinate

β – complex convective heat coefficient

γ – Biot numbers ratio

δ – dimensionless thickness

η – fin efficiency

θ – dimensionless fin temperature

θ_0 – dimensionless fin temperature, zero-order

θ_1 – dimensionless fin temperature, first-order

$\tilde{\theta}$ – average local dimensionless fin temperature in *r*-direction

λ – thermal conductivity

ξ – dimensionless thermo-geometrical fin parameter

References

[1] Bergles A.E. (1998): *Techniques To Enhance Heat Transfer*.– in Handbook of Heat Transfer, I., Eds., McGraw-Hill, New York.

[2] Bergles A.E. and Manglik R.M. (2013): *Current progress and new development in enhanced heat and mass transfer*.– Journal of Enhanced Heat Transfer, vol.20, pp.1-15, DOI:10.1615/JEnhHeatTransf.2013006989.

[3] Maji A. and Choubey G. (2020): *Improvement of heat transfer through fins: A brief review of recent developments*.– Heat Transfer, vol.49, No.3, pp.1658-1685, https://doi.org/10.1002/htj.21684.

[4] Nagarani N., Mayilsamy K., Murugesan A. and Kumar G.S. (2014): *Review of utilization of extended surfaces in heat transfer problems*.– Renewable and Sustainable Energy Reviews, vol.29, pp.604-613, https://doi.org /10.1016 /j.rser.2013.08.068.

[5] Tiari S., Hockins A. and Mahdavi M. (2021): *Numerical study of a latent heat thermal energy storage system enhanced by varying fin configurations*.– Case Studies in Thermal Engineering, vol.25, p.100999. https:// doi.org/10.1061/j.csite.2021.100999.

[6] Zhang S., Mancin S. and Pu L. (2023): *A review and prospective of fin design to improve heat transfer performance of latent thermal energy storage*.– Journal of Energy Storage, vol.62, p.106825, https://doi.org/10.1016 /j.est.2023.106825

[7] Yovanovich M.M., Culham J.R. and Lemczyk T.F. (1988): *Simplified solutions to circular annular fins with contact resistance and end cooling*.– Journal of Thermophysics and Heat Transfer, vol.2, No.2, pp.152-157, https://doi.org /10.2514/3.79.

[8] Gardner K.A. (1945): *Efficiency of extended surface.*– Transactions of The American Society of Mechanical Engineers, vol.67, No.8, pp.621-628, https://doi.org/10.1115/1.4018343.

[9] Harper D.R. and Brown W.B. (1922): *Mathematical equations for heat conduction in the fins of air-cooled engines.*– National Advisory Committee For Aeronautics. No.158, report. https://ntrs.nasa.gov/citations/19930091223

[10] Kraus A.D., Aziz A. and Welty J. (2001): *Extended Surface Heat Transfer.* Wiley, NewYork, https://doi.org /10.1115/1.1399680.

[11] Ozisik M.N (1993): *Heat Conduction*.– second ed. John Wiley and Sons, New York.

[12] Campo A., Acosta-Iborra A. and Masip-Macía Y. (2020): *Approximate analytical treatment of annular fins of rectangular profile for teaching fin heat transfer: Utilization of the mean value theorem for integrals.*– International Journal of Mechanical Engineering Education, vol.48(1), pp.79-96, https://doi.org/10.1177 /0306419018789336.

[13] Nellis G. and Klein S. (2008): *Heat Transfer*.– Cambridge University Press.

[14] Lau W. and Tan C.W. (1973): *Errors in one-dimensional heat transfer analysis in straight and annular fins*.– Journal of Heat Transfer, vol.95, p.549, https://doi.org/10.1115/1.3450110.

[15] Heggs P.J. and Stones P.R. (1980): *The effects of dimensions on the heat flow rate through extended surfaces*.– Journal of Heat Transfer, vol.101, p.180, https://doi.org/10.1115/1.3244236.

[16] Snider A.D. and Kraus A.D. (1983): *Recent developments in the analysis and design of extended surface.*– Journal of Heat Transfer, vol.105, p.302, https://doi.org/10.1115/1.3245578.

[17] Razelos P. and Georgiou E. (1992): *Two dimensional effects and design criteria for convective extended surfaces.*– Heat Transfer Engineering, vol.13, No.3, p.38, https://doi.org/10.1080/01457639208939780.

[18] Apparecido J.B and Cotta R.M. (1990): *Improved one-dimensional fin solution.*– Heat Transfer Engineering, pp.11-49, https://doi.org/10.1080/01457639008939722.

[19] Ju Y.H, Chou Y.S and Hsiao C.C. (1989): *A new approach to the transient conduction in a 2D rectangular fin.*– International Journal of Heat and Mass Transfer, vol.32, p.1657, https://doi.org/10.1016/0017-9310(89)90048-3.

[20] Cotta R.M and Ramos R. (1998): *Integral transforms in the two-dimensional non-linear formulation of longitudinal fins with variable profile.*– International Journal of Methods for Heat and Fluid Flow, vol.8, p.27, https:// doi.org/10.1108/09615539810197916.

[21] Bouaziz N. (2009): *Fin efficiency in 2D with convection at the tip and dissymmetry of exchange.*– Energy Conversion and Management, vol.50, No.6, pp.1618-1624, https://doi.org/10.1016/j.enconman.2009.02.011.

[22] Pires-Fonseca W.D. and Carrasco-Altemani C.A. (2024): *Experimental and numerical investigation of flat plate fins and inline strip fins heat sinks.*– Revista Facultad de Ingeniería Universidad de Antioquia, vol.110, pp.86-98, https: //www.doi.org/10.17533/udea.redin.20230417.

[23] Asgari M., Javidan M., Nozari M., Asgari A. and Ganji D.D. (2021): *Simulation of solidification process of phase change materials in a heat exchanger using branch-shaped fins.*– Case Studies in Thermal Engineering, vol.25, https://doi.org/10.1016/j.csite.2020.100835.

[24] Petrik M., Szepesi G. and Jarmai K. (2019): *CFD analysis and heat transfer characteristics of finned tube heat exchangers.*– Pollack Periodica, vol.14, No.3, pp.165-176, https://doi.org/10.1556/606.2020.15.3.9.

[25] Fayz-Al-Asad M., Sarker M.M.A. and Munshi M.J.H. (2019): *Numerical investigation of natural convection flow in a hexagonal enclosure having vertical fin*.– Journal of Scientific Research, vol.11, No.2, pp.173-183, https://doi.org/10.3329/jsr.v11i2.38797.

[26] Konar D., Sultan M.A. and Roy S. (2020): *Numerical analysis of 2-D laminar natural convection heat transfer from solid horizontal cylinders with longitudinal fins*.– International Journal of Thermal Sciences, vol.154, p.106391, https://doi.org/10.1016/j.ijthermalsci.2020.106391.

[27] Fourar I., Benmachiche A.H. and Abboudi S. (2021): *Effect of material and geometric parameters on natural convection heat transfer over an eccentric annular-finned tube*.– International Journal of Ambient Energy, vol.42, No.8, pp.929-939, https://doi.org/10.1080/01430750.2019.1573757.

[28] Lee J. H., Shin J.H., Chang S.M. and Min T. (2020): *Numerical analysis on natural convection heat transfer in a single circular fin-tube heat exchanger (Part1), numerical method*.– Entropy, vol.22, No.3, p.363, https://doi.org /10.3390 /e22030363.

[29] Gong J.H., Wang J., Lund P.D., Zhao D.D., Xu J. W. and Jin Y.H. (2021): *Comparative study of heat transfer enhancement using different fins in semi-circular absorber tube for large-aperture trough solar concentrator*.– Renewable Energy, vol.169, pp.1229-1241, http://dx.doi.org/10.1016/j.renene.2020.12.054.

[30] Durgam S., Kale A., Kene N., Khedkar A., Palve S. and Gawai N.M. (2021): *Thermal analysis of fin materials for engine cylinder heat transfer enhancement*.– In IOP Conference Series: Materials Science and Engineering, vol.1126, No.1, p.012071, http://dx.doi.org/10.1088/1757-899X/1126/1/012071.

[31] Sobamowo G. (2020): *Finite element thermal analysis of a moving porous fin with temperature-variant thermal conductivity and internal heat generation*.– Reports in Mechanical Engineering, vol.1, No.1, pp.110-127, http://dx.doi.org /10.31181/rme200101110s.

[32] Senthilkumar P., Babu S.R., Koodalingam B. and Dharmaprabhakaran T. (2020): *Design and thermal analysis on circular fin.*– Materials Today: Proceedings, vol.33, pp.2901-2906, http://dx.doi.org/10.1016/j.matpr.2020.02.784.

[33] Chitra J., Ananthaswamy V., Sivasankari S. and Sivasaundaram S. (2023): *A new approximate analytical method (ASM) for solving non-linear boundary value problem in heat transfer through porous fin.*– Mathematics in Engineering, Science and Aerospace, vol.14, No.1, pp.53-69, https://nonlinearstudies.com/index.php/mesa/ article/view/3058.

[34] Gireesha B. J. and Sowmya G. (2020): *Heat transfer analysis of an inclined porous fin using differential transform method.*– International Journal of Ambient Energy, vol.43, No.1, pp.3189-3195, http://dx.doi.org/10.1080/ 01430750.2020.1818619

[35] Hoseinzadeh S., Moafi A., Shirkhani A. and Chamkha A.J. (2019): *Numerical validation heat transfer of rectangular cross-section porous fins.*– Journal of Thermophysics and Heat Transfer, vol.33, No.3, pp.698-704, http://dx.doi.org /10.2514/1.T5583

[36] Sowmya G., Gireesha B.J., Khan M.I., Momani S. and Hayat T. (2020): *Thermal investigation of fully wet longitudinal porous fin of functionally graded material*.– International Journal of Numerical Methods for Heat and Fluid Flow, vol.30, No.12, pp.5087-5101, http://dx.doi.org/10.1108/HFF-12-2019-0908.

[37] Kundu B. and Yook S. J. (2021): *An accurate approach for thermal analysis of porous longitudinal, spine and radial fins with all nonlinearity effects-analytical and unified assessment*.– Applied Mathematics and Computation, vol.402, p.126124, http://dx.doi.org/10.1016/j.amc.2021.126124.

[38] Look Jr D.C. (1988): *Two-dimensional fin performance: Bi (top surface) ≥ Bi (bottom surface).*– Journal of Heat Transfer (Transactions of The American Society of Mechanical Engineers, series C), USA, vol.110, No.3, pp.780-782, https://doi.org/10.1115/1.3250559.

[39] Look Jr D.C. (1989): *Two-dimensional fin with non-constant root temperature.*– International Journal of Heat and Mass Transfer, vol.32, No.5, pp.977-980, https://doi.org/10.1016/0017-9310(89)90247-0.

[40] Look Jr D.C. and Kang H.S. (1991): *Effects of variation in root temperature on heat lost from a thermally non-symmetric fin.*– International Journal of Heat and Mass Transfer, vol.34, No.4-5, pp.1059-1065, https://doi.org/10.1016/0017-9310(91)90016-8.

[41]Look Jr D.C. and Kang H.S. (1992): *Optimization of a thermally non-symmetric fin-Preliminary evaluation.*– International Journal of Heat and Mass Transfer, vol.35, No.8, pp.2057-2060, https://doi.org/10.1016/0017-9310(92)90207-9.

[42] Kang H.S. and Look Jr D.C. (2001): *Thermally asymmetric triangular fin analysis.*– Journal of Thermophysics and Heat Transfer, vol.15, No.4, pp.427-430, https://doi.org/10.2514/2.6646.

[43] Kang H.S. and Look Jr D.C. (2004): *Thermally asymmetric annular rectangular fin optimization.*– Journal of Thermophysics and Heat Transfer, vol.18, No.3, pp.406-409, https://doi.org/10.2514/1.4951.

[44] Kang H.S. and Look Jr D.C. (2007): *Optimization of a thermally asymmetric convective and radiating annular fin.*– Heat Transfer Engineering, vol.28, No.4, pp.310-320, https://doi.org/10.1080/01457630601122609.

[45] Cheng C.Y. (1998): *Transient response of annular fins subjected to constant base temperatures.*– International Communications in Heat and Mass Transfer,– vol.25, No.6, pp.775-785, https://doi.org/10.1016/S0735-1933(98)00064-5.

[46] Mustafa M.T., Zubair S.M. and Arif A.F.M. (2011): *Thermal analysis of orthotropic annular fins with contact resistance: A closed-form analytical solution.*– Applied Thermal Engineering, vol.31, No.5, pp.937-945, https://doi.org /10.1016/j.applthermaleng.2010.11.017.

Received: April 14, 2024
Revised: August 7, 2024